Available online at www.sciencedirect.com
ScienceDirect
Ceramics International 37 (2011) 195–200
CERAMICS INTERNATIONAL
www.elsevier.com/locate/ceramint

# Gel-combustion, characterization and processing of porous Ni–YSZ cermet for anodes of solid oxide fuel cells (SOFCs)

M.B. Kakade [a,*], S. Ramanathan [a], D. Das [b]

[a] *Materials Processing Division, Bhabha Atomic Research Centre, Mumbai 4000 85, India*
[b] *Chemistry Division, Bhabha Atomic Research Centre, Mumbai 4000 85, India*

Received 7 May 2010; received in revised form 31 May 2010; accepted 21 August 2010
Available online 29 September 2010

**Abstract**

The NiO–YSZ powder was prepared by the combustion of nitrate–glycine gel, a novel and versatile technique to form the nano-composite. The phase purity of the as-formed powder was confirmed by XRD. Onset sintering temperature was measured and sintering of NiO–YSZ specimens was carried out at 1450 °C for different soaking times. Porosity of the specimens decreases with increasing soaking time. Ni–YSZ cermet with varying open porosities between 23 and 41% was obtained by the in situ reduction of NiO–YSZ. Electrical conductivity, thermal expansion coefficient, and SEM microstructure of the Ni–YSZ specimens possessing varying porosities were evaluated. The electrical conductivity decreased while thermal expansion coefficient remained essentially the same with increasing porosity. SEM results confirmed the presence of interconnected open pores.


*Keywords:* B. Porosity; B. Microstructure; C. Electrical conductivity; E. Fuel cells; Ni–YSZ cermet

## 1. Introduction

Solid oxide fuel cells an energy conversion system have generated great interest due to their higher energy efficiency and environmental friendship [1]. The basic elements of a typical fuel cell consist of an electrolyte which is in intimate contact with a porous cathode and a porous anode and each cell is separated by interconnect. The anode plays most important role to allow an oxidation of fuel to generate electricity. Presently, nickel–yttria stabilized zirconia cermet (Ni–YSZ) cermet is most widely used anode material for SOFC because of its good electro catalytic properties and low price [2]. The anode should have porous microstructure (porosity about 40%) which helps to diffuse gas readily to the anode/electrolyte interface and its thermal expansion should match with the other cell components. Therefore anode material should be stable in the reducing environment of the fuel.

Ni–YSZ anodes have been extensively studied because of their stability, conductivity, thermal expansion compatibility and catalytic activity [3–6]. The electrical property of Ni–YSZ cermet as an anode is greatly influenced not only by the electrical conductivity of each constituent component, but also by microstructural parameters like size, portion, spatial distribution and contiguity of each phase component. Pratihar et al. [7] reported that microstructural parameters are strongly dependent on powder preparation technique.

Ni–YSZ cermet can be fabricated by various methods. As the processing of a mixture of NiO and YSZ is easier than that of a Ni metal and an YSZ, the desired cermet is then obtained by in situ reduction of already processed NiO–YSZ composite. NiO–YSZ powder could be prepared by gel-combustion method. Gel-combustion is a simple technique for preparing nano-crystalline powders which involves heating the concentrated metal nitrates or oxy-nitrates solution with suitable fuel. Many authors have reported gel-combustion method for preparing NiO–YSZ powder. Marinsek et al. prepared NiO–YSZ by modified citrate–nitrate combustion synthesis and concluded that combustion process proceeded through several consecutive steps [8]. Kim et al. prepared NiO–YSZ by combustion method through control of pH and glycine content. After sintering and reduction treatment they studied the microstructure of Ni–YSZ pellet [9]. Huebner and Anderson

* Corresponding author. Tel.: +91 22 25590466; fax: +91 22 25505151.
*E-mail address:* mkakade@barc.gov.in (M.B. Kakade).

0272-8842/$36.00 
doi:10.1016/j.ceramint.2010.09.019

have studied the effect of pre-calcination temperature and vol.% of Ni on the conductivity, current density and microstructure of Ni–YSZ [10]. Marinsek et al. found that the precursor thermal decomposition properties depended on the citrate–nitrate ratio prior to the combustion [11].

In the present study Ni–YSZ specimens with graded porosities were made from gel-combustion synthesized NiO–YSZ powder. The changes observed in electrical conductivity, thermal expansion coefficient values and morphology of the Ni–YSZ specimens possessing varying porosities are presented.

## 2. Experimental

The anode material composition selected is {Ni–$[(ZrO_2)_{0.92}(Y_2O_3)_{0.08}]$} with Ni content of 50 vol.% and the ratio of oxides of NiO:$ZrO_2$:$Y_2O_3$ was 0.656:0.296:0.0474. The volume percent of the Ni phase was determined from the weight percent and density data for NiO and YSZ. The aqueous stock solutions of nickel nitrate (2.303 M), zirconium oxy-nitrate (3.10 M) and yttrium nitrate (2.388 M) desired for the above composition were mixed in a beaker. Fuel glycine in requisite amount was then added (glycine-to-nitrate molar ratio of ∼5/9 was used which is stoichiometric ratio). The solution was converted into high viscosity liquid by heating in an oven at 80–90 °C to remove the excess water and cooled to room temperature to form a gel. The precursor was formed by heating the gel in the beaker till the combustion reaction set in accompanied by the formation of foamy green powder. Typical combustion reaction between nickel nitrate, zirconium oxy-nitrate and yttrium nitrate with glycine fuel for the preparation of one mole of NiO and one mole of yttria stabilized zirconia composite can be given as:

$$\begin{aligned}&Ni(NO_3)_2 + 0.92ZrO(NO_3)_2 + 0.16Y(NO_3)_3 \\ &\quad + 2.35NH_2CH_2COOH \rightarrow NiO(0.92\ ZrO_2\ 0.08Y_2O_3) \\ &\quad + 4.69CO_2 + 3.33N_2 + 5.86H_2O\end{aligned} \quad (1)$$

As-formed NiO–YSZ precursor was planetary ball milled (M/s. Fritsch) to break the soft agglomerates to homogenize the precursor for about 15–20 min reducing thereby powder volume. The XRD pattern for the as-formed precursor was recorded in an X-ray diffractometer Model: Philips-1710. The as-formed precursor was calcined at 1350 °C for 1 h and was wet ground for 30 min. Laser light scattering method (Mastersizer 2000 from M/s. Malvern U. K.) was used to measure the average agglomerated particle size distribution of NiO–YSZ powders. 0.5 wt% polyethylene glycol was used as the binder for the fabrication of pellets and rectangular bars. Uni-axial method was used to fabricate pellets and rectangle bars at a pressure of 120 MPa from ground powder.

After binder burnout at 600 °C the pellets and rectangular bars were heated at a constant rate of heating at temperature between 1150 and 1550 °C (at an interval of 100 °C in between) without any soaking time to determine the onset sintering temperature. Sintering of the specimens was carried out at 1450 °C for the soaking time of 0.5–5 h. The density and open porosity of the sintered specimens were determined by liquid displacement method using water as a displaced liquid. Sintered NiO–YSZ specimens were converted into Ni–YSZ cermet by reduction treatment under hydrogen atmosphere at 1000 °C for 2 h. The hydrogen flow rate used was 10 l/h. XRD pattern for the Ni–YSZ cermet sample was recorded. The complete conversion of NiO was checked by calculating the expected and experimental weight loss or by measuring the total porosity of the specimen.

Electrical conductivity of the Ni–YSZ bar specimens with varying porosities was measured by four probe method at temperatures between room temperature to 950 °C on a laboratory assembled setup in a hydrogen atmosphere. The hydrogen flow rate used was 10 l/h. Platinum wires were used as current and potential leads. Current probes were configured at two ends (lengthwise) of a bar specimen. The voltage probes were configured by tightening wires at two points away from centre of the bar specimen. Platinum paste was applied between platinum wire and bar specimen for good contact. In four probe method known amount of current was supplied and the output voltage was measured. The range of current used was 540–590 mA and the range of voltage used was 1–5.5 mV.

Evaluation of thermal expansion coefficient behavior of selected sintered specimens up to 1000 °C was carried out in a dilatometer (Model TD 5000S Mac Science Co Ltd., Japan) at the heating rate of 6.7 °C/min in an argon atmosphere. Morphology of the Ni–YSZ specimens possessing varying amount of porosities were analyzed by SEM (Tescan-Vega MV-2300).

## 3. Results and discussion

### 3.1. Characterization of precursor/powder

The XRD pattern of the as-formed precursor is shown in Fig. 1. It showed patterns due to NiO and YSZ. This pattern matches with the XRD pattern of NiO–YSZ reported by Kim et al. [9] prepared by combustion method using glycine fuel. In gel-combustion compound formed is always a single phase

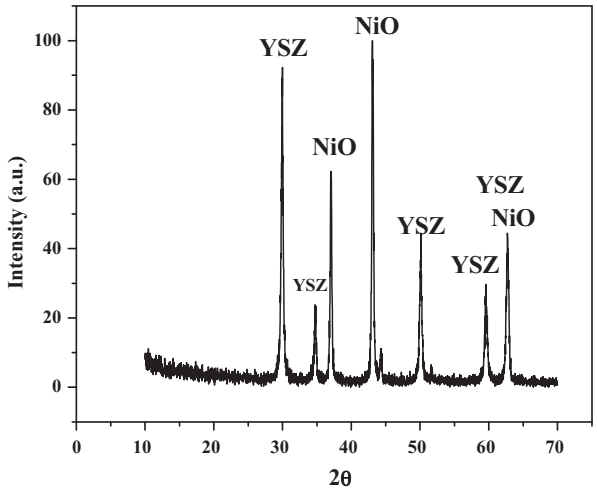


Fig. 1. XRD pattern of the as-formed NiO–YSZ precursor.

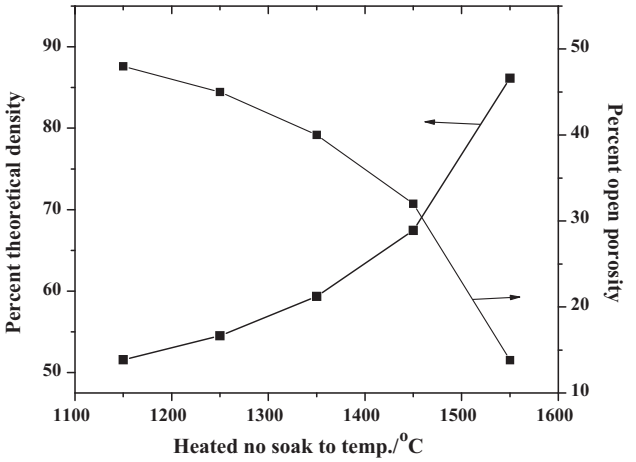


Fig. 2. Percent theoretical density and open porosity variation with temperature for the pellets and rectangular bars made from calcined NiO–YSZ powder.

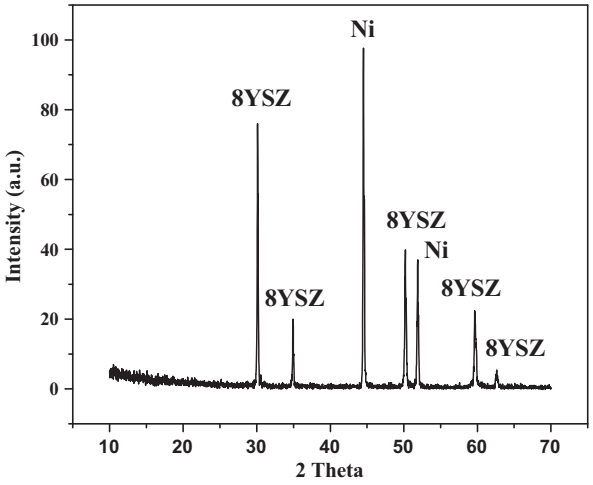


Fig. 3. XRD pattern of the Ni–YSZ cermet sample.

homogeneous oxide compound containing one or more metal atoms, but in the case of NiO–YSZ we obtained two phases mixture of NiO and YSZ. The reason is that the solubility of NiO in yttria stabilized zirconia has been reported to be below 2 mol% at 1600 °C. The solubility is increasing with increasing temperature [12]. In our study on the role of calcination temperatures on the NiO–YSZ powder characteristics and sintering behavior indicates that 1350 °C calcined powder possesses the desired property for sintering and undergoes minimum shrinkage which is required for the shape fabrication. Therefore 1350 °C calcined powder was selected in this study.

### 3.2. Onset sintering temperature of NiO–YSZ

The average agglomerated particle sizes of the as-formed, 1350 °C calcined and 30 min wet ground NiO–YSZ powders were 2.7, 6.4 and 3.0 μm, respectively. The temperature at which sintering process starts, that is onset of sintering, was measured. The variations of densities and porosities for the NiO–YSZ specimens against temperature at which they are heat treated without any soaking time are as shown in Fig. 2. It is seen from the figure that as the heating temperature of the specimen increased from 1150 to 1550 °C the percent theoretical density of the specimens increased while their porosity decreased. Above the temperature of 1450 °C sudden rise in density occurs.

### 3.3. Formation of porous Ni–YSZ specimens

At the temperature of 1500 °C, NiO evaporates from the system and in SOFC technology, fabrication work at such a high temperature is not permissible because there is possibility of migration of element like Mn of cathode material into the electrolyte. Therefore it was decided to carryout the sintering at 1450 °C for the period of different sintering time to fabricate the specimens with varying porosities. From the density–porosity data obtained, it was decided to select the sintering time of 0.5, 1, 2 and 5 h for this work. Thus sintered NiO–YSZ specimens with porosities values of 21, 13, 6.5 and 1.4% were obtained. The XRD pattern of the Ni–YSZ cermet sample is shown in Fig. 3. It showed pattern due to YSZ and contained some additional peaks around $2\theta$ values of 44.5° and 51.9° which were due to the presence of Ni particles. The principal peaks for Ni were at same $2\theta$ position as reported by Kim et al. [9]. In this pattern no NiO peaks appears which indicates that NiO is completely converted into Ni.

The variation of percent porosity observed before and after reduction with different sintering time (for NiO–YSZ specimens) is shown in Fig. 4. The lower curve showed the porosity of the NiO–YSZ specimens and the upper curve showed the porosity of the Ni–YSZ specimens after reduction. In these specimens, more or less same amount of additional porosity was created due to the conversion of NiO to Ni. The Ni–YSZ specimens after reduction treatment exhibited the graded porosities of 41, 34, 28 and 23%. The NiO–YSZ specimen which exhibited 21% porosity initially, after reduction it attained 41% porosity. The weight loss of the specimens during the reduction was due to the conversion of NiO to Ni and the created porosity corresponding to the oxygen loss.

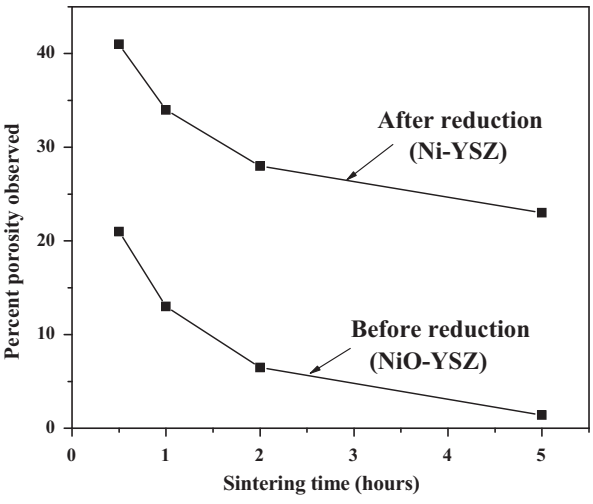


Fig. 4. Percent porosity observed with sintering time for the NiO–YSZ before and after reduction.

In anode supported design of SOFC, generally impervious YSZ layer formation is carried out on porous NiO–YSZ substrate. The NiO in the composite anode undergoes reduction to Ni at 1000 °C during SOFC operation. At 1000 °C the Ni formed does not undergo sintering. Therefore during fuel cell fabrication anode does not loose the porosity.

### 3.4. Characterization of porous bodies

#### 3.4.1. Electrical conductivity

The plot showing the change of electrical conductivity in the temperature range of 450–950 °C for the porous Ni–YSZ bar specimens is shown in Fig. 5. The Ni content being 50 vol.%, the conduction behavior of Ni–YSZ is metallic one as expected. As reported in the literature, if nickel content in Ni–YSZ is above 30 vol.%, the specimen shows metallic behavior that is the conductivity decreased with increasing temperature [1]. Metallic conductivity in Ni–YSZ cermet was achieved by the formation of Ni–Ni chains within the cermet matrix. For a Ni–YSZ cermet containing 50 vol.% Ni, the conductivity was through the Ni phase which was evident from the conductivity behavior observed. The conductivity value for the specimen (A), with 23% porosity was higher than the specimen (B), possessing 34% porosity, while specimen (C) with 41% porosity showed lowest conductivity value. For example, the conductivity value at 950 °C, for the specimen (A) exhibiting 23% porosity was 1072 S $cm^{-1}$, whereas for the specimens (B) and (C) with 34 and 41% porosities it was 906 and 817 S $cm^{-1}$, respectively at same temperature. The conductivity value decreased as the porosity of the specimen increased.

Similar trend of decrease in the conductivity with increasing temperature for Ni–YSZ specimen containing 50 vol.% Ni has been reported by Aruna et al. The 39% porous Ni–YSZ specimen exhibited a conductivity value 989 S $cm^{-1}$ at 900 °C [13]. We have observed that as the porosity in the specimen increased the contact points between the two neighboring grains or inter-connectivity between the grains decreased and it resulted in lowering in the conductivity of the specimen and it decreased

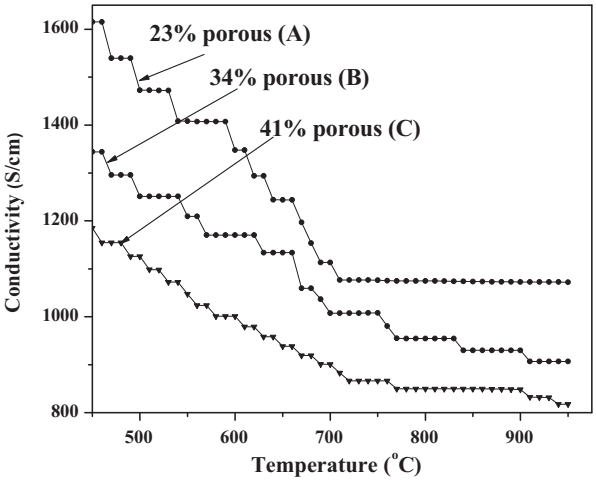


Fig. 5. Electrical conductivity variation with temperature for porous Ni–YSZ samples.

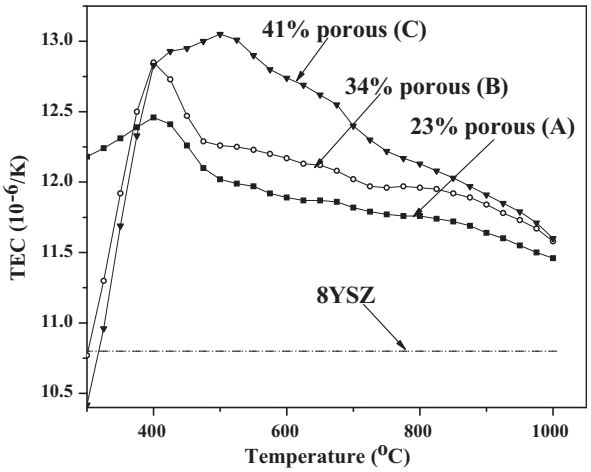


Fig. 6. Thermal expansion coefficient (TEC) of sintered porous Ni–YSZ samples as a function of temperature (TEC value of YSZ sample at 1000 °C is shown as dashed line).

further with increasing in porosity as has been observed for the LSM system [14]. The pore occupies the space where actually nickel particles would have been to provide electrical connection. The decrease in electrical conductivity with increasing porosity was correlated to the open microstructure. Similarly, Chen et al. observed that the conductivities of the Ni–YSZ anodes decreased with increasing porosity of the Ni–YSZ anode [15].

The electrical conductivity for the specimen (C) with 41% porosity during heating up to 950 °C and also during cooling cycle was determined. This showed that there was no change in the conductivity values of the specimens during heating and cooling schedule. Heat treating the specimen (C) exhibiting 41% porosity at 1000 °C for the soaking period of 100 h and the effect of heat treatment on the conductivity data was tested by measuring the conductivity. The conductivity data revealed that there was no change in the conductivity.

#### 3.4.2. Thermal expansion

The change in the thermal expansion coefficient (TEC) with temperature in the temperature range of 300–1000 °C for these specimens is shown in Fig. 6. The 8YSZ (electrolyte material) exhibited TEC value of 10.8 ppm $°C^{-1}$ at 1000 °C. The TEC value of yttria stabilized zirconia (8YSZ) is shown as a dashed line in the graph for comparison. It was observed that the TEC exhibited a peak at the Curie temperature of ~400 °C. The specimens with 23, 34 and 41% porosity at 1000 °C showed TEC values of 11.46, 11.58 and 11.6 ppm $°C^{-1}$, respectively. The value of 11.6 ppm $°C^{-1}$ is close to that reported for the electrolyte material YSZ satisfying the requirement for the composite structure of SOFC. A dilatometric study of the porous Ni–YSZ (porosity 26–40%) was carried out by Radovic et al. at temperature between 50 and 1000 °C in 4%$H_2$/96%Ar. They also found that the coefficients of thermal expansion of porous Ni–YSZ specimens were independent of porosity [16].

#### 3.4.3. Microstructural evaluation

The typical SEM micrographs of cross-section of porous Ni–YSZ specimens are shown in Fig. 7. The porosity in the

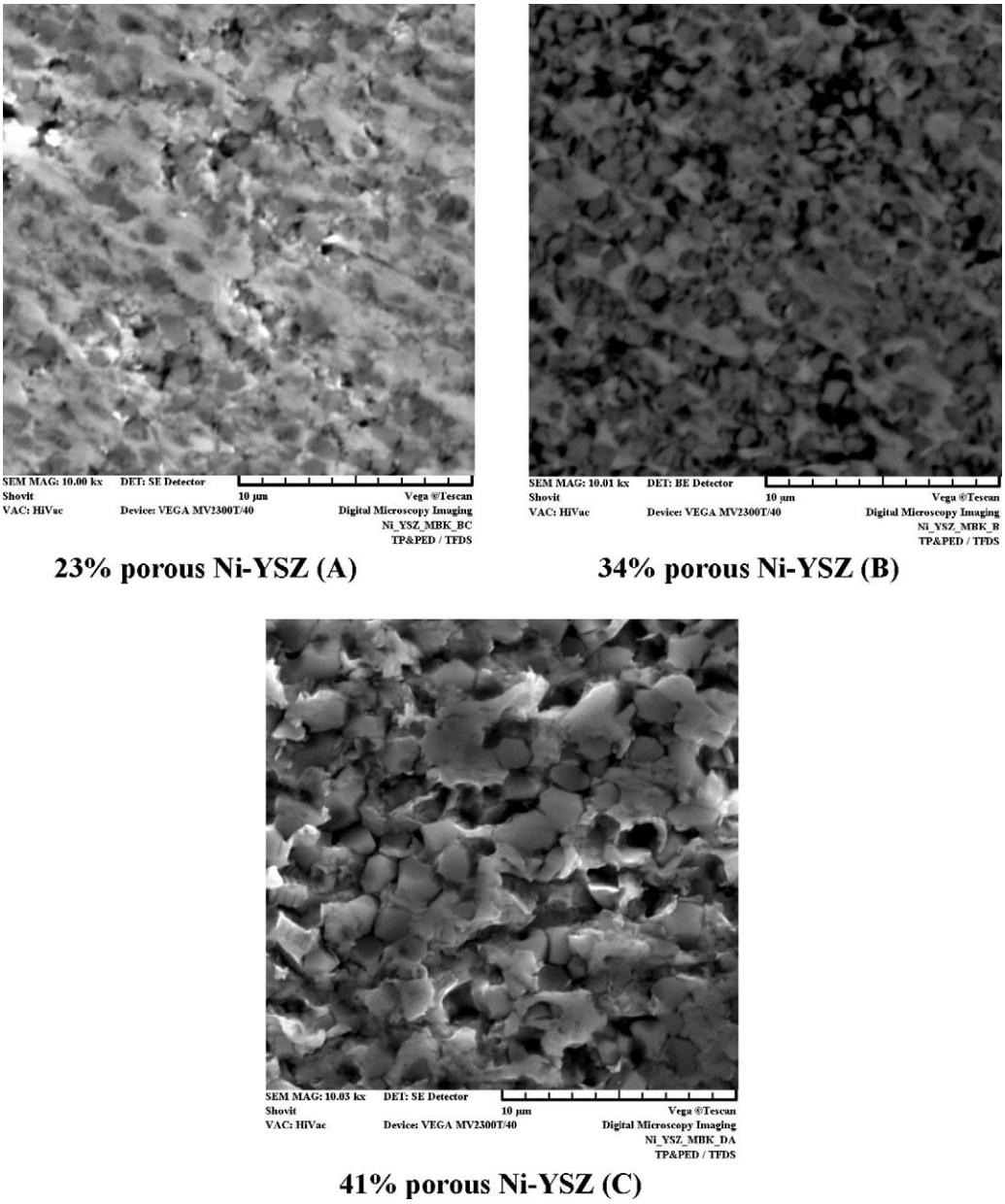


Fig. 7. SEM micrographs of cross-section of porous Ni–YSZ specimens.

specimen is clearly seen in micrographs. The specimens possessing 23, 34 and 41% porosities showed the desired interconnected porous structure containing well sintered Ni and YSZ grains. It is seen in the micrographs as the porosity of the specimen increases from 23 to 41% the interconnectivity between the grains decreases and this is responsible for lowering electrical conductivity of the specimen. The microstructural investigation by SEM of these specimens includes shape and size of the pores and their distribution, grain size and inter-grain connectivity.

In these micrographs the porosity is in the form of packets. The NiO–YSZ specimens possess porosity due to incomplete densification and the additional porosity in Ni–YSZ was due to the elimination of oxygen from NiO, therefore the resulting pores were of small size. The uniformly distributed fine grains and pores resulted in the sufficient triple phase boundaries.

Fukui et al. studied the morphology of Ni–YSZ cermet anodes, fired at 1200–1400 °C and reduced in $H_2$, by SEM and reported that morphology of Ni–YSZ cermet anode is changed with sintering temperature [17]. Huebner and Anderson reported the microstructure of 50 vol.% Ni compositions precalcined at 1400 °C and sintered on the YSZ electrolyte at different temperatures between 1300 and 1500 °C [10]. As expected, the average pore size of the specimen possessing 41% porosity was more than the average pore size of the other specimen. The average pore size of the specimens possessing 41 and 23% porosity were around 2 and 1 μm, respectively. The specimen exhibiting 41% porosity maintained the required interconnectivity of the particles as it was distinctly visible in the micrograph. The sintered specimen (41% porous) possessed the desired amount of porosity and interconnected grains structure which are requirements for the anode of SOFC.

## 4. Conclusions

The NiO–YSZ nano-composite powder was prepared by the combustion of nitrate–glycine gel. The appropriate sintering temperature was found to be 1450 °C.

NiO–YSZ specimens with graded porosities (between 1.4 and 21%) were generated by varying sintering time which upon reduction under hydrogen at 1000 °C resulted in the Ni–YSZ cermet with porosity in the range of 23–41%. The role of porosity on the electrical conductivity, thermal expansion and microstructure was evaluated.

The conductivity of Ni–YSZ specimens decreased with increasing porosity of the specimen. The decrease in electrical conductivity with increasing porosity was correlated to the open microstructure. The stability of the cermet for long time use for the SOFC applications was exhibited by the constant conductivity value of the cermet heated at 1000 °C up to 100 h. However, the thermal expansion coefficient of the Ni–YSZ composite was independent of the porosity. The morphology of the Ni–YSZ specimens confirms the presence of pores having average diameter of 1–2 μm forming interconnected open channels in the specimen containing well sintered Ni and YSZ grains.

## Acknowledgements

The authors thank Mr. Rakesh Shukla and Mr. A.D. Parmar of the Chemistry Division, Dr. S. Bhattacharya of Technical Physics & Prototype Engineering Division, Dr. A. Ghosh of Materials Processing Division, of BARC for their help with the XRD, electrical conductivity, SEM, dilatometer studies, respectively. Also the authors thank Dr. A.K. Suri, Director Materials Group and Dr. I.G. Sharma, Head, Material Processing Division for their keen interest in this work.

## References

[1] N.Q. Minh, J. Am. Ceram. Soc. 76 (3) (1993) 563–588.
[2] S.P.S. Badwal, K. Foger, Solid oxide fuel cell review, Ceram. Int. 22 (1996) 257–265.
[3] Y.M. Park, G.M. Choi, Solid State Ionics 120 (1999) 265–274.
[4] F. Tietz, F.J. Dias, D. Simwonis, D. Stover, J. Eur. Ceram. Soc. 20 (2000) 1023–1034.
[5] T. Fukui, K. Murata, S. Ohara, H. Abe, M. Naito, K. Nogi, J. Power Sources 125 (2004) 17–21.
[6] J.H. Lee, J. Heo, D.-S. Lee, J. Kim, G.-H. Kim, H.-W. Lee, H.S. Song, J.H. Moon, Solid State Ionics 158 (2003) 225–232.
[7] S.K. Pratihar, A. Dassharma, H.S. Maiti, Mater. Res. Bull. 40 (2005) 1936–1944.
[8] M. Marinsek, J.P. Gomilsek, I. Arcon, M. Ceh, A. Kodre, J. Macek, J. Am. Ceram. Soc. 90 (2007) 3274–3281.
[9] S.-J. Kim, W. Lee, W.J. Lee, J. Mater. Res. 16 (2001) 3621–3627.
[10] W. Huebner, H. U. Anderson, http://www.netl.doe.gov/publications/proceedings/97/97fc/FC61.PDF.
[11] M. Marinsek, Z. Klementina, J. Macek, J. Mater. Res. 18 (7) (2003) 1551–1560.
[12] A. Kuzjukevics, S. Linderoth, Solid State Ionics 93 (1997) 255–261.
[13] S.T. Aruna, M. Muthuraman, K.C. Patil, Solid State Ionics 111 (1998) 45–51.
[14] M.B. Kakade, S. Ramanathan, G.K. Dey, D. Das, Adv. Appl. Ceram. 107 (2) (2008) 89–95.
[15] K. Chen, Z. Lu, X. Chen, N. Ai, X. Huang, B. Wei, J. Hu, W. Su, J. Alloy Compd. 454 (2008) 447–453.
[16] M. Radovic, E. Lara-Curzio, R.M. Trejo, H. Wang, W.D. Porter, Advances in Solid Oxide Fuel Cells II, A John Wiley & Sons, INC., Publication, Hoboken, New Jersey, 2007, pp. 79–85.
[17] T. Fukui, S. Ohara, M. Naito, K. Nogi, J. Power Sources 110 (2002) 91–95.